The Astrophysical Journal, 781:92 (9pp), 2014 February 1 doi:10.1088/0004-637X/781/2/92

FREQUENCY AND DAMPING RATE OF FAST SAUSAGE WAVES

S. Vasheghani Farahani[1], C. Hornsey[2], T. Van Doorsselaere[1], and M. Goossens[1]
[1] Centre for Mathematical Plasma Astrophysics, Department of Mathematics, KU Leuven, Celestijnenlaan 200B bus 2400, B-3001 Heverlee, Belgium
[2] Centre for Fusion, Space, and Astrophysics, Physics Department, University of Warwick, Coventry CV4 7AL, UK
Received 2013 October 17; accepted 2013 December 10; published 2014 January 13

ABSTRACT

We investigate the frequency and damping rate of fast axisymmetric waves that are subject to wave leakage for a one-dimensional magnetic cylindrical structure in the solar corona. We consider the ideal magnetohydrodynamic (MHD) dispersion relation for axisymmetric MHD waves superimposed on a straight magnetic cylinder in the zero β limit, similar to a jet or loop in the solar corona. An analytic study accompanied by numerical calculations has been carried out to model the frequency, damping rate, and phase speed of the sausage wave around the cut-off frequency and in the long wavelength limit. Analytic expressions have been obtained based on equations around the points of interest. They are linear approximations of the dependence of the sausage frequency on the wave number around the cut-off wavelength for both leaky and non-leaky regimes and in the long wavelength limit. Moreover, an expression for the damping rate of the leaky sausage wave has been obtained both around the cut-off frequency and in the long wavelength limit. These analytic results are compared with numerical computations. The expressions show that the complex frequencies are mainly dominated by the density ratio. In addition, it is shown that the damping eventually becomes independent of the wave number in the long wavelength limit. We conclude that the sausage mode damping directly depends on the density ratios of the internal and external media where the damping declines in higher density contrasts. Even in the long wavelength limit, the sausage mode is weakly damped for high-density contrasts. As such, sausage modes could be observed for a significant number of periods in high-density contrast loops or jets.

Key words: magnetohydrodynamics (MHD) – Sun: corona – Sun: magnetic fields – waves

Online-only material: color figures

1. INTRODUCTION

Since the late 1990s, it has become clear that magnetohydrodynamic (MHD) waves are almost everywhere in the solar atmosphere. From a predominantly theoretical concept, they have evolved to a physical reality. An obvious starting point for a theoretical study of MHD waves on magnetic flux tubes was the analysis of linear MHD waves superimposed on a straight cylindrical plasma column with a constant longitudinal (vertical) magnetic field and a piecewise constant density. This analysis leads to two dispersion relations in terms of Bessel functions. Edwin & Roberts (1983) were not the first to document the dispersion relations but they complemented and extended previous work and gave a complete overview of the MHD waves given by these dispersion relations. Edwin & Roberts (1983) considered real frequencies ω and real longitudinal wave numbers k_z and supposed that there is no propagation of energy away or toward the cylinder at $r = R$. Edwin & Roberts (1983) confined their attention to the cylindrically symmetric (sausage or pulsational) modes given by $m = 0$ and the asymmetric (kink or taut-wire) modes given by $m = 1$.

Let us focus on the results of Edwin & Roberts (1983) for coronal loops shown in their Figure 4. An intriguing and shocking property of Figure 4 is that all dispersion curves, with one exception, of MHD waves with frequencies ω between the local internal Alfvén frequency ω_{Ai} and the local external Alfvén frequency ω_{Ae} have a low longitudinal wave number cut-off k_c. The dispersion curves do not start at $k_z = 0$ but at $k_z = k_c > 0$. The only exception is the radial fundamental mode of the kink waves (which was also discussed by Wentzel 1979), which is apparent from Figure 4 of Edwin & Roberts (1983). The cut-off longitudinal wave number k_c depends on the radial tone under consideration. The longitudinal cut-off wave number k_c does not mean that MHD waves with $k_z < k_c$ do not exist. Recall that Edwin & Roberts considered modes with ω and k_z both real, and hence excluded MHD waves with real k_z and complex frequencies. It was known first from plasma physics, geophysics, and later from solar physics that MHD waves can have complex frequencies even in ideal MHD when the background is non-uniform and the real part of the frequency is in the Alfvén continuum, i.e., in between the minimum and maximum value of the total Alfvén frequency. Even in a uniform plasma with resonant absorption absent, a linear MHD wave can have complex frequencies and undergo damping due to MHD radiation. This damping due to MHD radiation or leakage was first studied by Spruit (1982) both for axisymmetric ($m = 0$) and non-axisymmetric linear MHD waves; see also Cally (1986), Pascoe et al. (2007), Kopylova et al. (2007), and Nakariakov et al. (2012).

In non-uniform plasma, both resonant absorption and MHD radiation can lead to complex frequencies and damping. Damping of MHD waves by MHD radiation was first studied by Spruit (1982), and the combination of the resonant absorption and MHD radiation by Goossens & Hollweg (1993) and Stenuit et al. (1999).

The influence of resonant absorption and MHD radiation on the wave properties of the kink mode ($m = 1$) has been researched intensively by, e.g., Cally (1986), Ruderman & Roberts (2002), Goossens et al. (2002), Van Doorsselaere et al. (2004), Verwichte et al. (2006a), Brady et al. (2006), Verwichte et al. (2006b), Terradas et al. (2007), Arregui et al. (2008), Vasheghani Farahani et al. (2009), Soler et al. (2011), and Pascoe et al. (2012, 2013). However, less work has been done on the influence of resonant absorption or MHD radiation

on axisymmetric MHD waves, even though these waves are presumably more susceptible to MHD radiation compared with the kink mode (especially in the long wavelength limit). On the other hand, resonant absorption does not operate on axisymmetric MHD waves when the magnetic field is straight. It does work when an azimuthal magnetic field is included in addition to a longitudinal magnetic field, as explained by Sakurai et al. (1991) Goossens et al. (1992), and Goossens et al. (1995) and as seen in Figure 8 of Goossens & Poedts (1992). Here, we focus on the possible damping of the axisymmetric (or sausage) mode by MHD radiation. In order to keep the analysis as simple as possible, we consider the same equilibrium model as Edwin & Roberts (1983).

The study of MHD waves entered a new era when Roberts et al. (1984) stated that MHD waves may prove adequate for the diagnostics of the physical parameters of solar coronal plasmas (coronal seismology). Nakariakov et al. (2003) first claimed observational evidence of the sausage mode. They interpreted the 14–17 s quasi-periodic pulsations of an oscillating loop observed with the Nobeyama Radioheliograph in terms of the fundamental sausage mode (see also Melnikov et al. 2005). Srivastava et al. (2008) observed sausage oscillations in chromospheric cool post-flare loops with a measured period at the loop apex of about 587 s and foot points about 349 s. They interpreted the two different readings as indication of the fundamental and second harmonic oscillations of the sausage wave in chromospheric loops. Fujimura & Tsuneta (2009) reported the observation of sausage waves in the photosphere, where its applications to photospheric seismology were studied by Moreels & Van Doorsselaere (2013). Recently, oscillations with periods between 30 and 450 s observed in magnetic pores were interpreted as sausage waves (Morton et al. 2011). Standing fast and slow sausage waves were simultaneously observed in a flaring loop by Van Doorsselaere et al. (2011) having 75 and 8.5 s periods, respectively, which were used to estimate the plasma β. Forward modeling of the sausage mode was carried out by Gruszecki et al. (2012) and Antolin & Van Doorsselaere (2013).

In order to use the sausage mode for seismology, its dependence on the equilibrium parameters needs to be well understood. The geometric effects of the guiding structures were shown to change the period of oscillations of the fundamental sausage wave. A positive divergence in the loop cross section would decrease the wave period (Pascoe et al. 2009). Moreover, a transverse structuring in a magnetic slab in the form of a step function profile would also shift the period ratio of the sausage wave (Macnamara & Roberts 2011). Interestingly, the plasma β of the external and internal media does not affect the cut-off wave number (Inglis et al. 2009).

Recently, Nakariakov et al. (2012) performed a parametric numerical study in order to investigate the dependence of the sausage frequency on its wavelength for both trapped and leaky regimes. Their results show that as the wavelength becomes shorter, the period steadily increases. In the long wavelength limit, the period becomes independent of the wavelength. It was also deduced that the cut-off wavelength is proportional to the density ratio of external and internal media. Still, analytic expressions for sausage frequency and damping rate in the neighborhood of the cut-off frequency have not been obtained.

The aim here is to derive analytic expressions in the zero-β limit for the sausage wave frequency, damping rate, and phase speed on the longitudinal wave number in the leaky regime around the cut-off frequency. The results are also compared with those obtained numerically. The importance of studying the sausage wave in the leaky regime is to use it for coronal seismology.

2. MODEL AND EQUILIBRIUM CONDITIONS

We study axisymmetric ($m = 0$) MHD waves or sausage MHD waves superimposed on a straight static magnetic cylinder. The magnetic cylinder with radius a is embedded in a plasma medium with an equilibrium magnetic field (B_{z0}) in the direction of the cylinder axis. The equilibrium magnetic field is homogeneous because we consider the cold plasma limit ($\beta = 0$).

2.1. Solution at the Cut-off Wave Number k_c

Consider the perturbations of the physical parameters to be proportional to $\exp i(kz + m\varphi + \omega t)$. The dispersion relation for the sausage wave ($m = 0$) is

$$\frac{\rho_i}{\rho_e}\frac{\left(\omega_{Ai}^2-\omega^2\right)}{\left(\omega_{Ae}^2-\omega^2\right)}\frac{m_e}{n_i}=\frac{J_1(n_ia)K_0(m_ea)}{J_0(n_ia)K_1(m_ea)}, \tag{1}$$

with

$$m_e^2=\frac{k^2C_{Ae}^2-\omega^2}{C_{Ae}^2},\quad n_i^2=-\frac{k^2C_{Ai}^2-\omega^2}{C_{Ai}^2}, \tag{2}$$

where ρ is the piecewise constant density, k is the longitudinal wave number, ω is the complex frequency, and C_{Ai} and C_{Ae} are the internal and external Alfvén speeds, respectively; see Edwin & Roberts (1983).

The zeroth-order solution to Equation (1) at k_c is $\omega = \omega_{Ae} = k_cC_{Ae}$. In this case, the arguments of the second order modified Bessel function K become small and we can use their expansions for small arguments (Abramowitz et al. 1988)

$$K_0(m_ea)=-\ln\left(\frac{1}{2}m_ea\right),\qquad K_1(m_ea)=\frac{1}{m_ea}. \tag{3}$$

After substituting ρ_i/ρ_e by C_{Ae}^2/C_{Ai}^2, Equation (1) reduces to

$$\frac{C_{Ae}^2}{C_{Ai}^2}\frac{\left(\omega^2-\omega_{Ai}^2\right)}{\left(\omega^2-\omega_{Ae}^2\right)}\frac{m_e}{n_i}=-\frac{J_1(n_ia)}{J_0(n_ia)}m_ea\ln\left(\frac{1}{2}(m_ea)\right). \tag{4}$$

Hence, the argument of the Bessel function $J_0(n_ia)$ at k_c has to be the zero of a Bessel function; see also Khongorova et al. (2012). This allows us to calculate the cut-off wave number k_c to be

$$k_ca=\frac{C_{Ai}j_{0,1}}{\sqrt{C_{Ae}^2-C_{Ai}^2}}=\frac{j_{0,1}}{D}, \tag{5}$$

where $j_{0,1}$ is the first zero of the Bessel function $J_0(n_ia)$ and we have introduced a new notation for the factor depending on the density contrast

$$D^2=\frac{C_{Ae}^2}{C_{Ai}^2}-1=\frac{\rho_i}{\rho_e}-1=\zeta-1.$$

Here, we have also used the notation $\zeta = \rho_i/\rho_e$ as first introduced in Van Doorsselaere et al. (2004).

2.2. Leaky Regime to the Left of k_c in the Neighborhood of the Cut-off Wave Number

The dispersion relation for an outwardly propagating leaky sausage wave ($m = 0$) is

$$\frac{\rho_i}{\rho_e}\frac{\left(\omega_{Ai}^2-\omega^2\right)}{\left(\omega_{Ae}^2-\omega^2\right)}\frac{n_e}{n_i}=\frac{J_1(n_ia)H_0^{(2)}(n_ea)}{J_0(n_ia)H_1^{(2)}(n_ea)}, \tag{6}$$

where $H^2(n_e r) = J(n_e r) - IY(n_e r)$ is the outgoing wave solution; see Edwin & Roberts (1983) and Cally (1986). In the zero-β regime we have

$$n_e^2 = -\frac{k^2 C_{Ae}^2 - \omega^2}{C_{Ae}^2}. \tag{7}$$

In order to determine the frequency around the cut-off value, we write $\omega = \omega_{Ae} + \Delta\omega$ and $k = k_c + \Delta k$, and consider both $\Delta\omega$ and Δk as small quantities ($|\Delta k| \ll k_c$). From physical intuition, we know that the phase speed V must increase when $\Delta k < 0$ and thus $\Re(\Delta V) > 0$. By substituting these expressions in Equations (2) and (7), we obtain

$$\begin{aligned} n_e^2 &= \left(\frac{\omega_{Ae}^2 + 2\omega_{Ae}\Delta\omega - C_{Ae}^2 k_c^2 - 2k_c C_{Ae}^2 \Delta k}{C_{Ae}^2}\right) \\ n_i^2 &= \left(\frac{\omega_{Ae}^2 + 2\omega_{Ae}\Delta\omega - C_{Ai}^2 k_c^2 - 2k_c C_{Ai}^2 \Delta k}{C_{Ai}^2}\right), \end{aligned} \tag{8}$$

where terms with $(\Delta\omega)^2$ and $(\Delta k)^2$ have been neglected in comparison to linear or zeroth order terms. Since $\omega_{Ae} = C_{Ae}k_c$, the first and third term in the numerator of the expression for n_e in Equation (8) cancel each other out. Hence, the expression for n_e in terms of $\Delta\omega$ and Δk is

$$\begin{aligned} n_e = \sqrt{\frac{2\Delta e}{C_{Ae}^2}}, \quad \Delta e &= C_{Ae}k_c\Delta\omega - k_c C_{Ae}^2 \Delta k \\ &= \omega_{Ae}^2\left(\frac{\Delta\omega}{\omega_{Ae}} - \frac{\Delta k}{k_c}\right). \end{aligned} \tag{9}$$

We substitute $\omega_{Ae} = C_{Ae}k_c$ in the expression for n_i of Equation (8). Subsequently we factor out terms without $\Delta\omega$ and Δk. The resulting expression for n_i in terms of the small parameters $\Delta\omega$ and Δk is then

$$n_i = k_c D\,(1 + \Delta s)\,,$$

where

$$\begin{aligned} \Delta s &= \frac{C_{Ae}k_c\Delta\omega - k_c C_{Ai}^2\Delta k}{(C_{Ae}^2 - C_{Ai}^2)k_c^2} \\ &= \frac{1}{D^2}\left(\zeta\frac{\Delta\omega}{\omega_{Ae}} - \frac{\Delta k}{k_c}\right). \end{aligned} \tag{10}$$

Hence, the dispersion relation (Equation (6)) around the cut-off wave number is

$$\begin{aligned} C_{Ae}^2 \frac{k_c^2 D^2(1+2\Delta s)}{2\Delta e}\frac{\sqrt{\frac{2\Delta e}{C_{Ae}^2}}}{k_c D(1+\Delta s)} &= \\ -\left(\frac{J_0(k_c a D) - J_2(k_c a D)}{J_1(k_c a D)} + \frac{J_1(k_c a D)}{(k_c a D)\,J_1(k_c a D)\,\Delta s}\right) & \\ \times \frac{H_0^{(2)}\left(a\sqrt{\frac{2\Delta e}{C_{Ae}^2}}\right)}{H_1^{(2)}\left(a\sqrt{\frac{2\Delta e}{C_{Ae}^2}}\right)}. & \end{aligned} \tag{11}$$

To obtain Equation (11), we have used the Taylor expansion of the Bessel functions J_0 and J_1 about $k_c a D$. Since the cut-off point k_c is a zero of the Bessel J_0 in the internal medium (as shown in the previous subsection), we obtain

$$\begin{aligned} C_{Ae}D\frac{k_c(1+\Delta s)}{\sqrt{2\Delta e}} = &-\left(-\frac{J_2(k_c a D)}{J_1(k_c a D)} + \frac{1}{(k_c a D)\,\Delta s}\right) \\ &\times \left\{\frac{J_0\left(a\sqrt{\frac{2\Delta e}{C_{Ae}^2}}\right) - iY_0\left(a\sqrt{\frac{2\Delta e}{C_{Ae}^2}}\right)}{J_1\left(a\sqrt{\frac{2\Delta e}{C_{Ae}^2}}\right) - iY_1\left(a\sqrt{\frac{2\Delta e}{C_{Ae}^2}}\right)}\right\}. \end{aligned} \tag{12}$$

We use the expansions for the Bessel and Hankel functions (Abramowitz et al. 1988)

$$\begin{aligned} J_0(n_e a) &= 1 - \frac{1}{4}\left(a^2\frac{2\Delta e}{C_{Ae}^2}\right), \\ J_1(n_e a) &= \frac{1}{2}\left(a\sqrt{\frac{2\Delta e}{C_{Ae}^2}}\right), \\ Y_0(n_e a) &= \frac{2}{\pi}\ln\left(\frac{1}{2}a\sqrt{\frac{2\Delta e}{C_{Ae}^2}}\right), \\ Y_1(n_e a) &= \frac{-2}{\pi a\sqrt{\frac{2\Delta e}{C_{Ae}^2}}}, \end{aligned} \tag{13}$$

and substitute them in Equation (12). We neglect higher order terms to obtain

$$\begin{aligned} -C_{Ae}D^2k_c^2 a\left(\frac{1}{2}a\sqrt{\frac{2\Delta e}{C_{Ae}^2}} + i\frac{2C_{Ae}}{\pi a\sqrt{2\Delta e}}\right)\Delta s & \\ = \sqrt{2\Delta e}\left[1 - \frac{i}{\pi}\ln\left(\frac{a^2\Delta e}{2C_{Ae}^2}\right)\right]. & \end{aligned} \tag{14}$$

In order to eliminate Δe in the denominator of the left-hand side (LHS) of Equation (14), we multiply both sides by $\sqrt{2\Delta e}$, and therefore we obtain

$$\begin{aligned} -C_{Ae}D^2\left(\frac{a\Delta e}{C_{Ae}^2} + i\frac{2C_{Ae}}{\pi a}\right)\Delta s & \\ = \frac{2\Delta e}{k_c^2 a}\left[1 - \frac{i}{\pi}\ln\left(\frac{a^2\Delta e}{2C_{Ae}^2}\right)\right]. & \end{aligned} \tag{15}$$

We substitute the expressions for Δs and Δe to obtain

$$\begin{aligned} \left\{1 + i\frac{C_{Ae}^2}{\pi C_{Ai}^2} - \frac{i}{\pi}\ln\left[\frac{k_c^2 a^2}{2}\left(\frac{\Delta\omega}{\omega_{Ae}} - \frac{\Delta k}{k_c}\right)\right]\right\}\frac{\Delta\omega}{\omega_{Ae}} & \\ = \left\{1 + \frac{i}{\pi} - \frac{i}{\pi}\ln\left[\frac{k_c^2 a^2}{2}\left(\frac{\Delta\omega}{\omega_{Ae}} - \frac{\Delta k}{k_c}\right)\right]\right\}\frac{\Delta k}{k_c}. & \end{aligned} \tag{16}$$

Equation (16) is an implicit and complex dispersion relation for the complex frequency of the sausage mode. To proceed, we separate the real and imaginary parts of the frequency and write two (implicit) relations. Since the arguments of the logarithms in Equation (16) are complex, we use the logarithmic definition $\ln(x + iy) = (1/2)\ln(x^2 + y^2) + i\arctan(y/x)$. Thus the real and imaginary parts of the logarithmic terms are separated by

$$\begin{aligned} \ln\left\{\frac{k_c^2 a^2}{2}\left(\frac{\Delta\omega}{\omega_{Ae}} - \frac{\Delta k}{k_c}\right)\right\} &= i\arctan\left(\frac{\Im(\Delta\omega)}{\Re(\Delta\omega) - C_{Ae}\Delta k}\right) \\ &+ \frac{1}{2}\ln\left\{\left(\frac{k_c^2 a^2}{2}\right)^2\left[\left(\frac{\Re(\Delta\omega)}{\omega_{Ae}} - \frac{\Delta k}{k_c}\right)^2 + \left(\frac{\Im(\Delta\omega)}{\omega_{Ae}}\right)^2\right]\right\}. \end{aligned} \tag{17}$$

The imaginary part of the frequency corresponds to the damping of the wave. In combining Equations (16) and (17), the arctan term could be neglected compared to the second term, because the second term is the logarithm of a small quantity Δk, whereas the arctan term is linear in this small quantity. We define the real argument of the logarithm as

$$\Delta W = \left(\frac{k_c^2 a^2}{2}\right)^2 \left\{\left(\frac{\Re(\Delta\omega)}{\omega_{Ae}} - \frac{\Delta k}{k_c}\right)^2 + \left(\frac{\Im(\Delta\omega)}{\omega_{Ae}}\right)^2\right\}. \quad (18)$$

Equation (16) is written in the form

$$\frac{\Delta\omega}{\Delta k} = C_{Ae}\left[1 + \frac{i}{\pi} - \frac{i\ln(\Delta W)}{2\pi}\right] \times \left[1 + \frac{iC_{Ae}^2}{\pi C_{Ai}^2} - \frac{i\ln(\Delta W)}{2\pi}\right]^{-1}. \quad (19)$$

We multiply the denominator and numerator of Equation (19) by the complex conjugate of the denominator $(1-iC_{Ae}^2/(\pi C_{Ai}^2)+(i/2\pi)\ln(\Delta W))$, and obtain

$$\frac{\Delta\omega}{\Delta k} = C_{Ae}\left[1 + \frac{C_{Ae}^2}{\pi^2 C_{Ai}^2} - \frac{C_{Ae}^2}{2\pi^2 C_{Ai}^2}\ln(\Delta W) + \frac{1}{4\pi^2}(\ln(\Delta W))^2 + \frac{i}{\pi} - i\frac{C_{Ae}^2}{\pi C_{Ai}^2}\right] \times \left[1 + \frac{C_{Ae}^4}{\pi^2 C_{Ai}^4} + \frac{1}{4\pi^2}(\ln(\Delta W))^2 - \frac{C_{Ae}^2}{\pi^2 C_{Ai}^2}\ln(\Delta W)\right]^{-1}. \quad (20)$$

Note that the term $(1/2\pi^2)\ln(\Delta W)$ has been neglected in comparison to the term $(1/4\pi^2)[\ln(\Delta W)]^2$ when obtaining Equation (20), because we assume that $|\Delta\omega| \ll 1$. This neglection is based on the fact that the arguments of the logarithms are small so that the absolute value of the logarithm is large. Hence, the square of the logarithm would be much greater than the logarithm itself.

Finally, the dependence of the sausage mode frequency and the damping rate on the wave number could be defined by two coupled implicit equations as

$$\frac{\Re(\Delta\omega)}{\Delta k} = C_{Ae}\left[1 + \frac{C_{Ae}^2}{\pi^2 C_{Ai}^2} - \frac{C_{Ae}^2\ln(\Delta W)}{2\pi^2 C_{Ai}^2} + \frac{(\ln(\Delta W))^2}{4\pi^2}\right] \times \left[1 + \frac{C_{Ae}^4}{\pi^2 C_{Ai}^4} + \frac{(\ln(\Delta W))^2}{4\pi^2} - \frac{C_{Ae}^2\ln(\Delta W)}{\pi^2 C_{Ai}^2}\right]^{-1}. \quad (21)$$

$$\frac{\Im(\Delta\omega)}{\Delta k} = -\frac{C_{Ae}}{\pi}\left[\frac{C_{Ae}^2}{C_{Ai}^2} - 1\right] \times \left[1 + \frac{C_{Ae}^4}{\pi^2 C_{Ai}^4} + \frac{(\ln(\Delta W))^2}{4\pi^2} - \frac{C_{Ae}^2\ln(\Delta W)}{\pi^2 C_{Ai}^2}\right]^{-1} \quad (22)$$

for the frequency and damping rate. This system of equations is implicit and can be solved numerically.

2.2.1. Expressions for Low-density Contrast

In this section, we consider the case where the density contrast is not too high. In other words, we neglect the terms in $C_{Ae}^2/C_{Ai}^2 = \rho_i/\rho_e = \zeta$ in comparison with the logarithmic terms. The mathematical condition for this is $\zeta \ll \ln\Delta W$ or $\Delta W \ll \exp(-\zeta)$. Retaining only the terms containing $(\ln\Delta W)^2$ in Equation (21), we obtain an extremely simple expression for the frequency change:

$$\frac{\Re(\Delta\omega)}{\omega_{Ae}} = \frac{\Delta k}{k_c} \quad \text{or} \quad \frac{\Re(\Delta\omega)}{\Delta k} = C_{Ae}. \quad (23)$$

This equation physically means that the dispersion curve of the frequency of the sausage mode (real part of ω) is tangent to the line for the external Alfvén frequency at the location (and left) of the cut-off wave number.

Using this expression, we find a much simpler expression for ΔW:

$$\Delta W = \left(\frac{k_c^2 a^2}{2}\right)^2 \frac{\Im(\Delta\omega)^2}{\omega_{Ae}^2}, \quad (24)$$

because the part containing $\Re(\Delta\omega)$ exactly cancels out using Equation (23). In Equation (22) we can also neglect all terms other than $(\ln\Delta W)^2$ (as for obtaining Equation (23)). The equation then reduces to

$$\frac{\Im(\Delta\omega)}{\Delta k} = -\frac{4\pi C_{Ae}}{(\ln\Delta W)^2}\left(\frac{C_{Ae}^2}{C_{Ai}^2} - 1\right). \quad (25)$$

Using Equation (24) (and the definition of D), this equation can be rewritten as

$$\frac{\Im(\Delta\omega)}{\omega_{Ae}}\left(\ln\frac{\Im(\Delta\omega)^2}{\omega_{Ae}^2}\right)^2 = -4\pi D^2\frac{\Delta k}{k_c}. \quad (26)$$

Let us now introduce two auxiliary variables

$$X = -\ln\frac{\Im(\Delta\omega)^2}{\omega_{Ae}^2} \quad \text{and} \quad \eta = -4\pi D^2\frac{\Delta k}{k_c} > 0. \quad (27)$$

Here $X \gg 1$ and $\eta \ll 1$. Equation (26) then can be written as

$$X^2\sqrt{\exp(-X)} = \eta. \quad (28)$$

This transcendental equation can easily be solved numerically. It turns out that this equation has two roots (for positive X), one of which is close to $X = 0$ and the other one large. Since $X \gg 1$, we disregard the small solution and concentrate on the large one. Let us denote the large solution as $X(\eta)$.

We can thus obtain the explicit solution for the damping of the sausage mode in the neighborhood of the cut-off wave number:

$$\frac{\Im(\Delta\omega)}{\Delta k} = -\frac{4\pi C_{Ae}}{X(\eta)^2}\left(\frac{C_{Ae}^2}{C_{Ai}^2} - 1\right). \quad (29)$$

We have numerically calculated the solutions to Equation (29), and have displayed them in Figure 1.

2.2.2. Expressions for High-density Contrast

Let us now consider the other case when the logarithmic term may be ignored in comparison with the density contrast. Such an asymptotic solution may be relevant for high-density

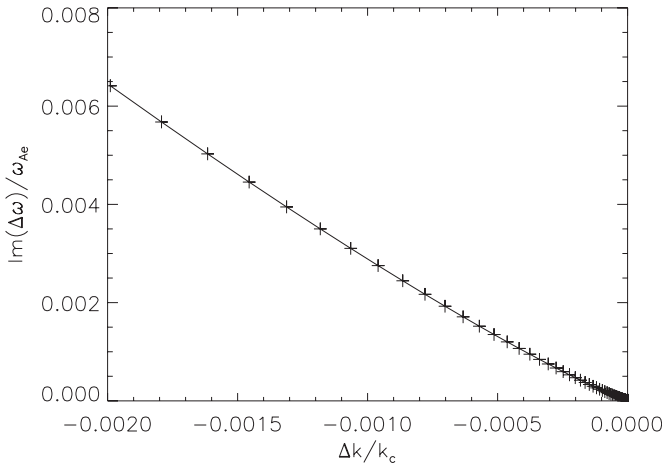

Figure 1. Imaginary part of the frequency as a function of the wave number calculated for a density contrast of $\rho_i/\rho_e = 5$, using formula (29).

jets (Cirtain et al. 2007), for very dense coronal loops, or for chromospheric structures (where Morton et al. 2012 recently measured the cut-off wave number for sausage modes). We again try to simplify the expressions for the frequency (Equation (21)) and damping (Equation (22)) of the sausage mode to explicit equations. Hence, we consider the density ratios as $\rho_e/\rho_i = (C_{Ae}^2/C_{Ai}^2)^{-1} \ll 1$ and terms without C_{Ae}^2/C_{Ai}^2 may be neglected. Equations (21) and (22) then reduce to the simpler versions

$$\frac{\Re(\Delta\omega)}{\Delta k} \approx \frac{C_{Ai}^2}{C_{Ae}}\left\{1 - \frac{1}{2}\ln\left[\frac{k_c^4 a^4}{4}\left(\left[\frac{\Re(\Delta\omega)}{\omega_{Ae}} - \frac{\Delta k}{k_c}\right]^2 + \left[\frac{\pi C_{Ai}^2}{C_{Ae}^2}\frac{\Delta k}{k_c}\right]^2\right)\right]\right\}, \tag{30}$$

for the frequency of the leaky sausage mode, and

$$\frac{\Im(\Delta\omega)}{\Delta k} = -\frac{\pi C_{Ai}^2}{C_{Ae}}, \tag{31}$$

for the damping rate of the sausage mode. Indeed, $\Im(\Delta\omega) > 0$ if $\Delta k < 0$, showing that we obtain a damped mode for wave numbers smaller than the cut-off wave number k_c.

To obtain Equation (31), we have neglected the logarithmic term in Equation (16) compared to ρ_e/ρ_i. This implies

$$-\frac{C_{Ae}^2}{C_{Ai}^2} \ll \ln\left(\frac{k_c^2 a^2}{2}\left|\frac{\Delta\omega}{\omega_{Ae}} - \frac{\Delta k}{k_c}\right|\right). \tag{32}$$

By exponentiating both sides, we obtain

$$\frac{2}{k_c^2 a^2}\exp\left(-\frac{C_{Ae}^2}{C_{Ai}^2}\right) \ll \left|\frac{\Delta\omega}{\omega_{Ae}} - \frac{\Delta k}{k_c}\right| \ll 1. \tag{33}$$

Therefore, the condition on $\Delta\omega$ and Δk must comply to Equation (33), to neglect the logarithmic term, and $\Delta\omega$ and Δk must be sufficiently large. Physically, this means that there is a small region around the cut-off where the (real part of the) dispersion curve follows the Alfvén frequency (Equation (23)), but as we gradually move to higher values of $|\Delta k|$, Equation (30) becomes more appropriate and the dispersion curve diverges from the Alfvén frequency. The expressions derived in this subsection are only valid sufficiently (but also not too far) away from the cut-off wave number.

The equivalent of Equation (30) in the sense of the variations of the phase speed with respect to the wave number could be either obtained by the same process as for the frequency, where the phase speed V is also expanded around the cut-off frequency ($V = C_{Ae} + \Delta V$), or by the direct relation between $\Delta\omega$ and ΔV which is

$$\frac{\Delta\omega}{\Delta k} = k_c\frac{\Delta V}{\Delta k} + C_{Ae}. \tag{34}$$

This results in

$$\frac{\Re(\Delta V)}{\Delta k} \approx \frac{C_{Ai}^2}{k_c C_{Ae}} - \frac{C_{Ae}}{k_c} - \frac{C_{Ai}^2}{2k_c C_{Ae}}\ln\left\{\frac{k_c^4 a^4}{4}\left(\left[\frac{\Re(\Delta V)}{C_{Ae}}\right]^2 + \left[\frac{\pi C_{Ai}^2}{C_{Ae}^2}\frac{\Delta k}{k_c}\right]^2\right)\right\}. \tag{35}$$

The terms with C_{Ai}^2 can be neglected for high density contrasts in comparison to C_{Ae}^2, which leaves

$$\frac{\Re(\Delta V)}{\Delta k} \approx -\frac{C_{Ae}}{k_c}. \tag{36}$$

Note that the condition of Equation (33) applies here as well.

2.3. Leaky Regime in the Long Wavelength Limit

At this stage, it is interesting to look at the dependence of the sausage wave frequency and damping rate on the wave number in the long wavelength limit ($k \to 0$). The dispersion relation of (Equation (6)) at $k = 0$ is

$$\frac{\rho_i}{\rho_e}\frac{\left(\omega_{Ai}^2 - \omega_0^2\right)}{\left(\omega_{Ae}^2 - \omega_0^2\right)}\frac{n_e}{n_i} = \frac{J_1(n_i a)H_0^{(2)}(n_e a)}{J_0(n_i a)H_1^{(2)}(n_e a)}, \tag{37}$$

where $\omega_0 = \omega(k = 0)$ is the complex solution at $k = 0$. Following the same procedure as around the cut-off, we obtain

$$\begin{aligned}\frac{C_{Ae}\left(1+\frac{\Delta A}{2}\right)}{C_{Ai}\left(1+\frac{\Delta Ae}{2}\right)} = {} & \frac{\left[J_1\left(\frac{\omega_0 a}{C_{Ai}}\right) + \frac{\omega_0 a}{2C_{Ai}}\left(J_0\left(\frac{\omega_0 a}{C_{Ai}}\right) - J_2\left(\frac{\omega_0 a}{C_{Ai}}\right)\right)\Delta A\right]}{\left[J_0\left(\frac{\omega_0 a}{C_{Ai}}\right) - \frac{\omega_0 a}{C_{Ai}}J_1\left(\frac{\omega_0}{C_{Ai}}a\right)\Delta A\right]} \\ & \times\left[J_0\left(\frac{\omega_0 a}{C_{Ae}}\right) - \frac{\omega_0 a}{C_{Ae}}J_1\left(\frac{\omega_0 a}{C_{Ae}}\right)\Delta Ae - iY_0\left(\frac{\omega_0 a}{C_{Ae}}\right)\right. \\ & \left. + i\frac{\omega_0 a}{C_{Ae}}Y_1\left(\frac{\omega_0 a}{C_{Ae}}\right)\Delta Ae\right]\left[J_1\left(\frac{\omega_0 a}{C_{Ae}}\right)\right. \\ & \left. + \frac{\omega_0 a}{2C_{Ae}}\left\{J_0\left(\frac{\omega_0 a}{C_{Ae}}\right) - J_2\left(\frac{\omega_0 a}{C_{Ae}}\right)\right\}\Delta Ae - iY_1\left(\frac{\omega_0 a}{C_{Ae}}\right)\right. \\ & \left. - i\frac{\omega_0 a}{2C_{Ae}}Y_0\left(\frac{\omega_0 a}{C_{Ae}}\right)\Delta Ae + i\frac{\omega_0 a}{2C_{Ae}}Y_2\left(\frac{\omega_0 a}{C_{Ae}}\right)\Delta Ae\right]^{-1}, \end{aligned} \tag{38}$$

and

$$\Delta Ae = \frac{2\omega_0\Delta\omega - C_{Ae}^2(\Delta k)^2}{\omega_0^2}, \quad \Delta A = \frac{2\omega_0\Delta\omega - C_{Ai}^2(\Delta k)^2}{\omega_0^2}. \tag{39}$$

The parameters ΔA and ΔAe have been obtained in the same way as Δs. In this case, the zeroth order dispersion relation is

$$\frac{C_{Ae}}{C_{Ai}} = \frac{J_1\left(\frac{\omega_0 a}{C_{Ai}}\right)}{J_0\left(\frac{\omega_0 a}{C_{Ai}}\right)} \times \frac{J_0\left(\frac{\omega_0 a}{C_{Ae}}\right) - iY_0\left(\frac{\omega_0 a}{C_{Ae}}\right)}{J_1\left(\frac{\omega_0 a}{C_{Ae}}\right) - iY_1\left(\frac{\omega_0 a}{C_{Ae}}\right)}. \tag{40}$$

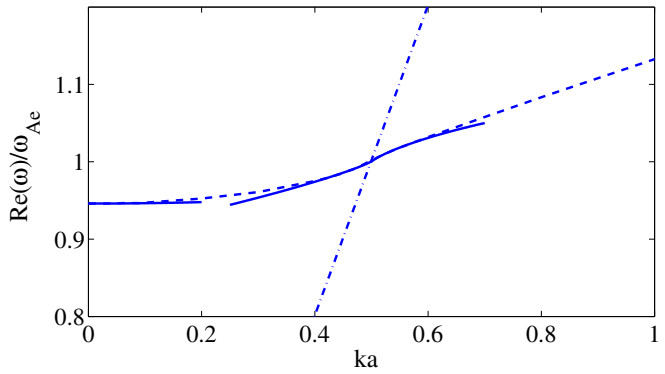

Figure 2. Frequency variations of the sausage oscillations around the cut-off frequency and in the long wave length limit are shown. The solid lines show the approximated analytic expressions in the leaky (Equation (30)) and non-leaky regimes (Equation (55)) regimes around the cut-off wave number, together with its dependence in the long wavelength limit (Equation (45)). The dashed line shows the frequency calculated numerically considering an initial value problem. The dash-dotted line shows the external Alfvén frequency. The density ratio $\rho_i/\rho_e = C_{Ae}^2/C_{Ai}^2$ has been taken 25. All frequencies have been normalized by the external Alfvén frequency at the cut-off.

(A color version of this figure is available in the online journal.)

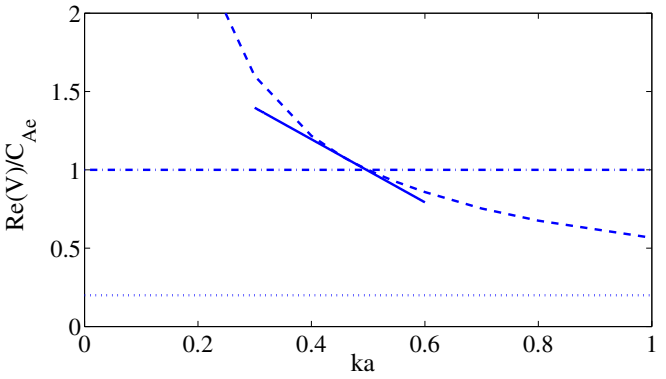

Figure 3. Phase speed variation of the sausage wave around the cut-off frequency is shown. The solid line shows the approximation obtained for the leaky and non-leaky regimes by Equation (35) taking the density ratio $\rho_i/\rho_e = C_{Ae}^2/C_{Ai}^2$ equal to 25. The speeds are normalized by the external Alfvén speed. The dashed line shows the sausage mode phase speed calculated by the numerical solution of the initial value problem. The dash-dotted and the dotted lines represent the external and internal Alfvén speeds, respectively.

(A color version of this figure is available in the online journal.)

By substituting values for C_{Ai} and C_{Ae} corresponding to various density contrasts in the corona, we obtain the exact value for ω_0.

In this case, analytical progress is only possible for a high-density contrast. We recall Equation (38) to consider higher order terms. Multiply the denominator of the right-hand side (RHS) with the numerator of the LHS of Equation (38) and vice versa, and consider the values of the Bessel functions at $k = 0$. Terms linear (or higher order) in $\rho_e/\rho_i \ll 1$ are neglected. Hence we obtain

$$\frac{1}{2}J_0\left(\frac{\omega_0 a}{C_{Ai}}\right)J_0\left(\frac{\omega_0 a}{C_{Ae}}\right)\Delta Ae - \frac{C_{Ae}}{C_{Ai}}J_1\left(\frac{\omega_0 a}{C_{Ai}}\right)J_1\left(\frac{\omega_0 a}{C_{Ae}}\right)\Delta A + i\frac{C_{Ae}}{C_{Ai}}J_1\left(\frac{\omega_0 a}{C_{Ai}}\right)Y_1\left(\frac{\omega_0 a}{C_{Ae}}\right)\Delta A = 0. \quad (41)$$

In this domain, the real and imaginary parts of ω_0 (normalized by ω_{Ae}) are smaller than unity, and these values are obtained by numerically solving Equation (40). The results also show that the real part of ω_0 is much larger than the imaginary part of ω_0; see Figures 2 and 4. Now, by substituting the limiting expressions for the Bessel functions as

$$J_0 = 1 - \frac{(\omega_0 a)^2}{4C_{Ai,e}^2}, \quad J_1 = \frac{1}{2}\frac{\omega_0 a}{C_{Ai,e}}, \quad \text{and} \quad Y_1 = -\frac{2C_{Ae}}{\pi\omega_0}, \quad (42)$$

and substituting terms for ΔA and ΔAe, we obtain

$$\left(\omega_0 - \frac{3\omega_0^3 a^2}{4C_{Ai}^2} + \frac{\omega_0^5 a^4}{16C_{Ai}^2 C_{Ae}^2} - i\frac{2C_{Ae}^2\omega_0}{\pi C_{Ai}^2}\right)\Delta\omega = \left(\frac{1}{2}C_{Ae}^2 - \frac{\omega_0^2 a^2 C_{Ae}^2}{8C_{Ai}^2} + \frac{\omega_0^4 a^4}{32C_{Ai}} - i\frac{C_{Ae}^2}{\pi}\right)(\Delta k)^2. \quad (43)$$

By solving the zeroth order dispersion relation (Equation (40)) numerically, we find that for coronal conditions the imaginary part of ω_0 is much smaller than its real part; see Figures 2 and 4. Thus, in writing ω_0 in terms of its real and imaginary parts, terms with $\Im(\omega_0)$ can be neglected in comparison to $\Re(\omega_0)$. Hence, Equation (43) could be simplified to

$$\frac{\Delta\omega}{(\Delta k)^2} = \left(\frac{C_{Ae}^2}{2} - \frac{(\Re(\omega_0))^2 a^2 C_{Ae}^2}{8C_{Ai}^2} - i\frac{C_{Ae}^2}{\pi}\right) \times \left(\Re(\omega_0) - \frac{3a^2}{4C_{Ai}^2}(\Re(\omega_0))^3 - i\frac{2C_{Ae}^2}{\pi C_{Ai}^2}\Re(\omega_0)\right)^{-1}. \quad (44)$$

We eliminate the imaginary terms in the denominator by multiplying the numerator and denominator with the complex conjugate of the denominator. Hence, an explicit expression for the frequency dependence on the wave number is obtained

$$\frac{\Re(\Delta\omega)}{(\Delta k)^2} = \frac{\pi^2 C_{Ai}^4}{8C_{Ae}^2\Re(\omega_0)}\left(1 + \frac{4C_{Ae}^2}{\pi^2 C_{Ai}^2} - \frac{(\Re(\omega_0))^2 a^2}{C_{Ai}^2}\right), \quad (45)$$

and the expression for the damping is

$$\frac{\Im(\Delta\omega)}{(\Delta k)^2} = \left(\frac{\pi C_{Ai}^2}{4C_{Ae}^2\Re(\omega_0)}\right) \times \left(C_{Ae}^2 - \frac{C_{Ae}^2(\Re(\omega_0))^2 a^2}{4C_{Ai}^2} + \frac{3(\Re(\omega_0))^2 a^2}{4}\right). \quad (46)$$

$\Re(\omega_0)$ and $\Im(\omega_0)$ are, respectively, the real and imaginary parts of the frequency ω_0 at $k = 0$.

It can readily be seen that the density contrast and consequently the ratio of the internal and external Alfvén frequencies controls the variations of the leaky frequencies and damping. This is illustrated in Figure 2 for the frequency and in Figure 3 for the speed. In Figure 4, the dependencies of the damping on the wave number is shown around the cut-off wavelength and the long wavelength limit. The solid lines in all figures refer to the linear approximations and the dashed lines show the numerical solutions to the initial value problem.

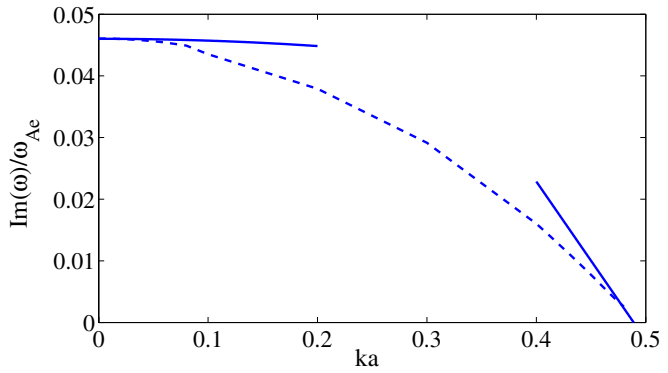

Figure 4. Solid lines show the damping of the sausage waves in the leaky regime plotted around the cut-off frequency using Equation (31) and the long wavelength limit using Equation (46). These curves are compared with the damping described by the numerical solution of the initial value problem, which is the dashed curve. The density ratio $\rho_i/\rho_e = C_{Ae}^2/C_{Ai}^2$ has been taken equal to 25. The damping has been normalized by the external Alfvén frequency at the cut-off.

(A color version of this figure is available in the online journal.)

2.4. Non-leaky Regime to the Right of and around the Cut-off Frequency

The dispersion relation for the non-leaky regime is (Edwin & Roberts 1983)

$$\frac{\rho_i}{\rho_e}\frac{\left(\omega_{Ai}^2-\omega^2\right)}{\left(\omega_{Ae}^2-\omega^2\right)}\frac{m_e}{n_i}=\frac{J_1(n_ia)K_0(m_ea)}{J_0(n_ia)K_1(m_ea)}, \tag{47}$$

with

$$m_e^2=\frac{k^2C_{Ae}^2-\omega^2}{C_{Ae}^2}, \tag{48}$$

where m_e^2 is positive. In this case, the sausage wave is trapped and there is no MHD radiation. We proceed as in the case of the leaky regime. We use Taylor expansions of $J_0(n_ia)$ and $J_1(n_ia)$ to obtain

$$\begin{aligned}C_{Ae}^2\frac{D^2k_c^2(1+2\Delta s)}{(-2\Delta e)}&\frac{\sqrt{\frac{-2\Delta e}{C_{Ae}^2}}}{k_cD(1+\Delta s)}\\&=\left(\frac{J_0\left(k_caD\right)-J_2\left(k_caD\right)}{J_1\left(k_caD\right)}+\frac{J_1\left(k_caD\right)}{\left(k_caD\right)J_1\left(k_caD\right)\Delta s}\right)\\&\quad\times\frac{K_0\left(a\sqrt{\frac{-2\Delta e}{C_{Ae}^2}}\right)}{K_1\left(a\sqrt{\frac{-2\Delta e}{C_{Ae}^2}}\right)}.\end{aligned} \tag{49}$$

The first term on the RHS of Equation (49) disappears because $\omega_{Ae}=k_cC_{Ae}$ is a zero for J_0 as explained in Section 2.1. We proceed in a similar manner as for the leaky regime and neglect higher order terms and substitute the limiting expressions for the Bessel functions. We keep in mind that the argument of the second order modified Bessel function is small, and we obtain

$$C_{Ae}^2D^2k_c^2\Delta s=2\Delta e\,\ln\left(\frac{1}{2}a\sqrt{\frac{-2\Delta e}{C_{Ae}^2}}\right), \tag{50}$$

where we have used (Abramowitz et al. 1988)

$$\begin{aligned}K_0(m_ea)&=-\ln\left(\frac{1}{2}m_ea\right)+\left[-\frac{1}{4}\ln\left(\frac{1}{2}m_ea\right)+\frac{1}{4}\right]m_e^2a^2\ldots\\K_1(m_ea)&=\frac{1}{m_ea}+\frac{1}{2}\ln\left(\frac{1}{2}m_ea-\frac{1}{4}\right)m_ea+\cdots.\end{aligned} \tag{51}$$

By substituting expressions for Δs and Δe and rearranging the terms, we obtain

$$\begin{aligned}&\left[\frac{C_{Ae}^2}{C_{Ai}^2}-\ln\left(\frac{k_c^2a^2}{2}\left|\frac{\Delta\omega}{\omega_{Ae}}-\frac{\Delta k}{k_c}\right|\right)\right]\Delta\omega\\&\quad=C_{Ae}\left[1-\ln\left(\frac{k_c^2a^2}{2}\left|\frac{\Delta\omega}{\omega_{Ae}}-\frac{\Delta k}{k_c}\right|\right)\right]\Delta k.\end{aligned} \tag{52}$$

Hence, the frequency as a function of the wave number in the non-leaky regime and close to the cut-off frequency would be

$$\begin{aligned}\frac{\Delta\omega}{\Delta k}&=C_{Ai}^2C_{Ae}\left[1-\ln\left(\frac{k_c^2a^2}{2}\left|\frac{\Delta\omega}{\omega_{Ae}}-\frac{\Delta k}{k_c}\right|\right)\right]\\&\quad\times\left[C_{Ae}^2-C_{Ai}^2\ln\left(\frac{k_c^2a^2}{2}\left|\frac{\Delta\omega}{\omega_{Ae}}-\frac{\Delta k}{k_c}\right|\right)\right]^{-1}.\end{aligned} \tag{53}$$

In the low density contrast limit (i.e., terms with ρ_i/ρ_e are neglected in comparison with the logarithmic term, see Section 2.2.1), we again obtain a similar result as Equation (23):

$$\frac{\Delta\omega}{\Delta k}=C_{Ae}, \tag{54}$$

where we now find that the imaginary part of the frequency is (of course) exactly equal to 0. In the non-leaky regime, the sausage mode is not damped. This was already known before.

If we once again consider the limit $\rho_e/\rho_i \ll 1$, the term with C_{Ai}^2 in the denominator could be neglected

$$\frac{\Delta\omega}{\Delta k}\approx-\frac{C_{Ai}^2}{C_{Ae}}\ln\left(\frac{k_c^2a^2}{2}\left|\frac{\Delta\omega}{\omega_{Ae}}-\frac{\Delta k}{k_c}\right|\right). \tag{55}$$

Note that the condition on $\Delta\omega$ and Δk must be

$$\frac{2}{k_c^2a^2}\exp\left(-\frac{C_{Ae}^2}{C_{Ai}^2}\right)\ll\left|\frac{\Delta\omega}{\omega_{Ae}}-\frac{\Delta k}{k_c}\right|\ll\frac{2}{k_c^2a^2}\exp\left(-1\right), \tag{56}$$

to allow the neglection of the logarithmic term in Equation (53). As in Section 2.2.2, these expressions are only valid far enough away from the cut-off wavelength.

2.5. Numerical Solutions and Discussions

The approximations for the expressions for the phase speed both for the leaky and non-leaky regimes have been plotted in Figure 2 and compared to numerical solutions of the one-dimensional wave equation. This wave equation was obtained from the linearized ideal MHD equations for a zero-β plasma cylinder, then a Fourier transform was taken in the longitudinal direction, and azimuthal symmetry was assumed. The evolution of an initial perturbation was then studied using a standard (2nd order) numerical solver. More details on the solution method can be found in Nakariakov et al. (2012).

For a density contrast of $\rho_i/\rho_e = C_{Ae}^2/C_{Ai}^2 = 25$, the numerical results are in agreement with our theoretical expressions. For a clearer illustration, the phase speed variation of the sausage wave around the cut-off wave number is plotted using the approximation obtained in Equation (35); see Figure 3. The solid

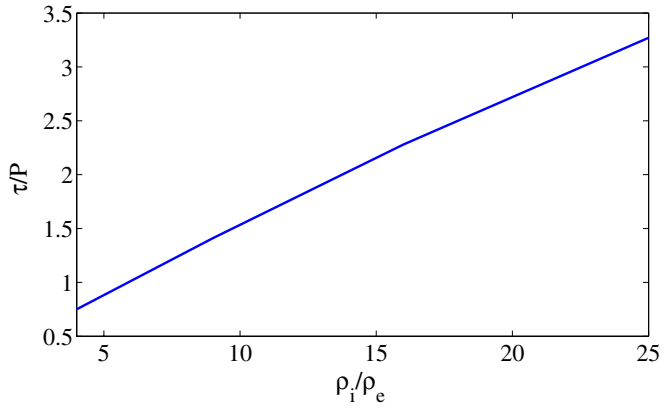

Figure 5. Ratio of the damping time and period is plotted for various density ratios with the wavelength fixed at $ka = 0$.

(A color version of this figure is available in the online journal.)

line approximates very well the numerical solution to the initial value problem for the sausage wave phase speed. In Figure 4, the damping rate of the leaky sausage wave has been plotted using Equation (31) and compared with the numerical results. In the regimes of applicability, the analytical formulae agree very well with the numerically obtained results. The results from Section 2.2.1 are not visible in the numerical results since the used density contrast is very high. It can be easily seen from Figure 4 that the damping rate becomes independent of the wave number as the wave number decreases.

An important quantity to study is the ratio of the damping time τ to the period P, which can be calculated by $\tau/P = \Re(\omega)/2\pi\Im(\omega)$. Of course, it is only useful to study this quantity in the leaky regime. When considering wave numbers greater than the cut-off wave number k_c, the sausage mode is confined to the cylinder and has infinite damping time. No MHD radiation takes place in this case.

For wave numbers smaller than the cut-off wave number k_c (i.e., longer wavelengths), the MHD mode gradually leaks away introducing an imaginary part of the frequency, and thus a finite damping time τ. For the density contrast of $\rho_i/\rho_e = 25$, the values for τ/P can be readily calculated by taking the ratio of the data in Figures 2 and 4 (and dividing by 2π). In the long wavelength limit ($ka \to 0$ and $\rho_i/\rho_e = 25$), the damping time takes an approximate value of $\tau/P \approx 3$, meaning that the amplitude of the sausage wave decreases by a factor e in three periods. When going to shorter wavelengths (higher ka), the mode is better confined and the damping time τ/P increases, approaching infinity when the wave number approaches the cut-off wave number ($ka \to k_c a \Rightarrow \tau/P \to \infty$). This means that, for the high density contrast flux tube we have studied, the sausage waves survive long enough to be observable in principle (subject to the limitations outlined in Antolin & Van Doorsselaere 2013).

In Figure 5, we have displayed the damping times as a function of density contrast, for a fixed value of $ka = 0$ (strongest leakage, lowest τ/P). It is clear that the statement that the sausage mode is observed for at least some periods is not always true. For low density contrasts, the sausage mode is heavily damped, as can be seen from the values of τ/P that drop below 1. In such a case, the energy leaks rapidly away from the cylinder by MHD radiation, resulting in a decrease of the wave amplitude by a factor 3 in just one period.

From Figure 5, we can predict that sausage modes can only be observed in very dense loops with a density contrast of a least $\rho_i/\rho_e = 20$, when the damping time is higher than three periods. The effects of finite spatial and temporal resolution should be taken into account when searching for sausage mode events (Antolin & Van Doorsselaere 2013).

3. CONCLUSIONS

We have performed an analytical study accompanied by numerical simulations in order to explain the behavior of the sausage wave in linear ideal MHD close to the cut-off frequency in the zero-β regime. We have obtained analytical expressions for the frequency, phase speed, and damping of the sausage waves ($m = 0$) around the cut-off frequency in addition to expressions for the sausage wave frequency and damping in the long wavelength limit. The model studied here is a straight untwisted and non-rotating magnetic cylinder embedded in a magnetic medium which resembles a coronal jet or loop, etc.

Analytic expressions have been obtained using various asymptotic techniques emphasizing behavior of the sausage wave just around the cut-off frequency both in the leaky and non-leaky regime (Equations (53) and (30)). The obtained equations show a very good agreement with the numerical results with similar coronal parameters. In addition to the frequency, the phase speed of the leaky sausage wave was also studied and an analytical expression was obtained (Equation (35)). The curves plotted with the use of the analytical expressions fitted well with the numerical results. In addition, analytical expressions for the damping of the sausage wave in the leaky regime around the cut-off wave number and in the long wavelength limit have been obtained (Equations (31) and (46)). Comparison of the damping curves plotted using Equation (31) and the numerical solution of the initial value problem showed good agreement.

The analytical expressions for the frequency and damping rate show how they are controlled by the density ratio of the internal and external media. In the long wavelength limit, the damping rate eventually becomes independent of the wave number. As the wave number tends to zero, the damping rate tends to a limiting value. This study of wave leakage by sausage modes has applications in coronal seismology. Morton et al. (2012) recently measured the cut-off frequency. The equations in this work could be used to obtain information about the density ratios and hence the Alfvén speed ratios of the coronal loops or jets and their exterior may be obtained.

For flux tubes of low density contrasts, the sausage mode cannot be observed, because the wave energy rapidly leaks away in less than a period. However, we have found that MHD radiation does not operate strongly on sausage modes if the density contrast is high enough. For loops or jets with a density contrast of $\rho_i/\rho_e \geqslant 20$, the damping time is at least three periods. In principle, the sausage mode could be observed for some periods in such high-density contrast loops.

T.V.D. acknowledges funding from an FWO Odysseus grant. S.V.F. acknowledges funding from the GOA/2009-009 of the KU leuven Research Council. This research has been funded by the Interuniversity Attraction Poles program initiated by the Belgian Science Policy office (IAP P7/08 CHARM). The authors thank the referee, M. Ruderman, for his constructive comments, especially in obtaining the results in Section 2.2.1.

REFERENCES

Abramowitz, M., Stegun, I. A., & Romer, R. H. 1988, AmJPh, 56, 958
Antolin, P., & Van Doorsselaere, T. 2013, A&A, 555, A74

Arregui, I., Terradas, J., Oliver, R., & Ballester, J. L. 2008, ApJL, 682, L141
Brady, C. S., Verwichte, E., & Arber, T. D. 2006, A&A, 449, 389
Cally, P. S. 1986, SoPh, 103, 277
Cirtain, J. W., Golub, L., Lundquist, L., et al. 2007, Sci, 318, 1580
Edwin, P. M., & Roberts, B. 1983, SoPh, 88, 179
Fujimura, D., & Tsuneta, S. 2009, ApJ, 702, 1443
Goossens, M., Andries, J., & Aschwanden, M. J. 2002, A&A, 394, L39
Goossens, M., & Hollweg, J. V. 1993, SoPh, 145, 19
Goossens, M., Hollweg, J. V., & Sakurai, T. 1992, SoPh, 138, 233
Goossens, M., & Poedts, S. 1992, ApJ, 384, 348
Goossens, M., Ruderman, M. S., & Hollweg, J. V. 1995, SoPh, 157, 75
Gruszecki, M., Nakariakov, V. M., & Van Doorsselaere, T. 2012, A&A, 543, A12
Inglis, A. R., van Doorsselaere, T., Brady, C. S., & Nakariakov, V. M. 2009, A&A, 503, 569
Khongorova, O. V., Mikhalyaev, B. B., & Ruderman, M. S. 2012, SoPh, 280, 153
Kopylova, Y. G., Melnikov, A. V., Stepanov, A. V., Tsap, Y. T., & Goldvarg, T. B. 2007, AstL, 33, 706
Macnamara, C. K., & Roberts, B. 2011, A&A, 526, A75
Melnikov, V. F., Reznikova, V. E., Shibasaki, K., & Nakariakov, V. M. 2005, A&A, 439, 727
Moreels, M. G., & Van Doorsselaere, T. 2013, A&A, 551, A137
Morton, R. J., Erdélyi, R., Jess, D. B., & Mathioudakis, M. 2011, ApJL, 729, L18
Morton, R. J., Verth, G., Jess, D. B., et al. 2012, NatCo, 3, 1315
Nakariakov, V. M., Hornsey, C., & Melnikov, V. F. 2012, ApJ, 761, 134
Nakariakov, V. M., Melnikov, V. F., & Reznikova, V. E. 2003, A&A, 412, L7
Pascoe, D. J., Hood, A. W., de Moortel, I., & Wright, A. N. 2012, A&A, 539, A37
Pascoe, D. J., Hood, A. W., De Moortel, I., & Wright, A. N. 2013, A&A, 551, A40
Pascoe, D. J., Nakariakov, V. M., & Arber, T. D. 2007, A&A, 461, 1149
Pascoe, D. J., Nakariakov, V. M., Arber, T. D., & Murawski, K. 2009, A&A, 494, 1119
Roberts, B., Edwin, P. M., & Benz, A. O. 1984, ApJ, 279, 857
Ruderman, M. S., & Roberts, B. 2002, ApJ, 577, 475
Sakurai, T., Goossens, M., & Hollweg, J. V. 1991, SoPh, 133, 247
Soler, R., Oliver, R., & Ballester, J. L. 2011, ApJ, 726, 102
Spruit, H. C. 1982, SoPh, 75, 3
Srivastava, A. K., Zaqarashvili, T. V., Uddin, W., Dwivedi, B. N., & Kumar, P. 2008, MNRAS, 388, 1899
Stenuit, H., Tirry, W. J., Keppens, R., & Goossens, M. 1999, A&A, 342, 863
Terradas, J., Andries, J., & Goossens, M. 2007, A&A, 469, 1135
Van Doorsselaere, T., Andries, J., Poedts, S., & Goossens, M. 2004, ApJ, 606, 1223
Van Doorsselaere, T., De Groof, A., Zender, J., Berghmans, D., & Goossens, M. 2011, ApJ, 740, 90
Vasheghani Farahani, S., Van Doorsselaere, T., Verwichte, E., & Nakariakov, V. M. 2009, A&A, 498, L29
Verwichte, E., Foullon, C., & Nakariakov, V. M. 2006a, A&A, 446, 1139
Verwichte, E., Foullon, C., & Nakariakov, V. M. 2006b, A&A, 449, 769
Wentzel, D. G. 1979, A&A, 76, 20